Nanoprobe study of the electric field driven insulator-to-metal transition in GaMo4S8

H. Koussir, Isabelle Lefebvre, Maxime Berthe, Y. Chernukha, J. Tranchant, B. Corraze, Etienne Janod, Laurent Cario, B. Grandidier, Pascale Diener

HAL Id: hal-03753819
https://hal.science/hal-03753819

Submitted on 18 Aug 2022

Nanoprobe study of the electric field driven insulator-to-metal transition in $GaMo_4S_8$

H. Koussir[1], **I. Lefebvre**[1], **M. Berthe**[1], **Y. Chernukha**[1], **J.Tranchant**[2], **B. Corraze**[2], **E. Janod**[2], **L. Cario**[2], **B. Grandidier**[1] and **P. Diener**[1]

[1] Univ. Lille, CNRS, Centrale Lille, Univ. Polytechnique Hauts-de-France, Junia-ISEN, UMR 8520 - IEMN, F-59000 Lille, France
[2] Institut des Matériaux Jean Rouxel (IMN), Université de Nantes, CNRS, 2 Rue de la Houssinière, BP32229, 44322 Nantes Cedex 3, France

E-mail: `pascale.diener@junia.com`

Abstract.   The resistive switching observed under electric pulses in Mott materials has a high potential for micro and nanoelectronics. Here we report on the study of the resistive switching observed at the surface of single crystals of the canonical Mott semiconductor $GaMo_4S_8$. The study is made using a multiprobe setup with 4 nanopositionable tips under the supervision of a high resolution scanning electron microscop. We find a resistivity of $38\,\Omega.cm$ by four-point probe measurements, in agreement with the literature. The volatile insulator to metal transition is studied with a two probes configuration for interelectrode distances varying between 4 and 200 microns. Finite element simulations are performed to determine the spatial distribution of the electric field prior to the transition. Our results are in agreement with i) an intrinsic voltage threshold of 60 mV independent of the interelectrode distance ii) a maximum electric field close to the electrodes and iii) a threshold electric field of 0.2 kV/cm.

Introduction

Mott materials exhibit an amazingly rich physics, with interesting perspectives for the micro/nanoelectronics industry [1, 2, 3]. This paper focuses on the electric field driven, volatile, insulator to metal transition observed in canonical narrow gap (0.1 - 0.5 eV) Mott insulators [4]. A voltage pulse induces an electronic avalanche specific to Mott insulators that allows the out of equilibrium system to explore a metastable metallic state [5]. The specific dynamics of the system is used to implement integrated artificial neurons [6]. In this context, the study of the transition at the nanoscaleis of high importance for the downscaling of future Mottronic devices using this transition.

Results

The $GaMo_4S_8$ single crystals are obtained using the method described in [5]. They are cleaved and glued with a conductive epoxy to a gold plated, p-doped silicon substrate. We checked that the sample substrate interface is sufficiently resistive in order to have a negligible contribution of the substrate to all measured sample resistances. The electrical properties have been obtained using the Nanoprobe, which consist of four Scanning Tunneling Microscop (STM) tips in an ultra high vacuum chamber, monitored under the supervision of a high resolution scanning electron microscop (SEM). The sharp tungsten tips are prepared using an electrochemical etching, and

annealed under vacuum to ensure a metallic apex. To check the quality of the tip-sample contact, current voltage measurements between each tip and the grounded substrate are performed and only tips showing a linear characteristic, associated with an ohmic contact, were considered. The sample resistance R_S is measured with the four-point probe method to avoid additional contact resistances, and with the sample substrate disconnected from the ground. Figure 1a shows a
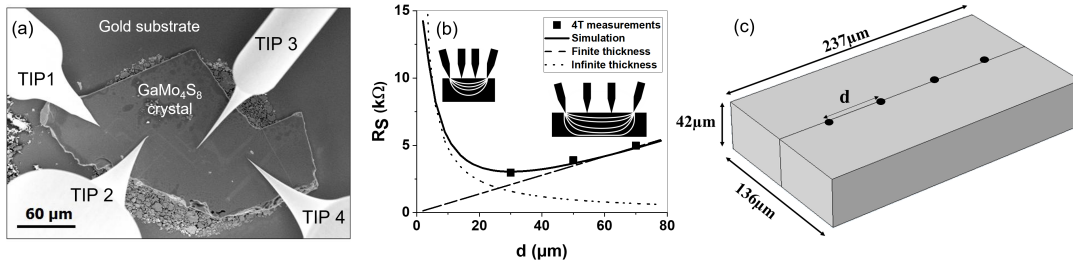

Figure 1. a) SEM picture of the GaMo$_4$S$_8$ single crystal S1 and the tips in the four-point probe configuration. b) Sample resistance R_S as a function of the interelectrode distance d. The experimental data are compared to simulations and to the expected analytic dependence at small d (*Infinite thickness*) and large d(*Finite thickness*). The insert shows a picture of the lines of current. c) Sample geometry used for COMSOL simulations.

typical SEM picture of a single crystal and the four STM tips. Figure 1b exhibits the variation of R_S in sample S1 for several interelectrode distances d from 30 to $70\,\mu m$. The resistance is expected to increase linearly with interelectrode distance for large values of d, and to decrease such as $R \propto 1/d$ for small d values [9]. These two limiting behaviour are pictured in Figure 1b: the first corresponds to the finite thickness case and the second corresponds to the semi infinite thickness case. Our data are expected to be in between the two regimes because the thickness is of the order of d.

Finite element simulations with COMSOL Multiphysics have been performed to fit the data, with the sample resistivity as a free parameter. Figure 1c show the sample geometry used for the simulations. The best fit, shown in Fig. 1b is obtained using a resistivity of $38\,\Omega cm$. This value is in excellent agreement with the resistivity of $40\,\Omega cm$ reported previously on single crystals of the same batch [5]. We have also compared four probes measurements $R_{4P} = R_S$ and two probes measurements $R_{2P} = R_S + 2R_c$ at the same position to estimate the contact resistance R_c at tip-sample interfaces. We find a reproducible $R_c \simeq 300k\Omega$. This value is well above the typical values ($< 1k\Omega$) obtained with the same setup on equivalent narrow gap semiconductors. Such a high contact resistance may be due to the presence of interface states specific to strongly correlated electronic systems, as discussed in [10].

We now focus on the electrical response of the sample at higher voltage using a two probes configuration and the sample floating. Figure 2a shows a typical current voltage curve measured at the surface of a GaMo$_4$S$_8$ single crystal. Transitions appear as a saturation of the current at threshold voltages $V^* = \pm12,0\,V$. V^* has been measured for two samples, S2 and S3, and for different interelectrode distances. As the measurements are performed with a two probes configuration, the voltage V_S across the sample differs from V^*, due to the potential drop at the contacts. Figure 2b gives the equivalent circuit of the measured resistance between the two electrodes, $R = R_S + 2R_C$, and indicates the measured voltage threshold V^* and the voltage threshold inside the sample V_S^*. V_S^* is calculated from the voltage divider relationship $V_S^* = V^*.R_S/R$. R is determined from a linear fit in the low field, ohmic regime, as shown in the insert of Figure 1a. R_S is determined from the simulation of the resistance in S2 and S3 following the procedure used for sample S1, with the same resistivity value.

Figure 2 (c-d-e) show R, V^* and V_S^* as a function of the interelectrode distance d. In the two probes configuration, the relatively high total resistance, above $600\,k\Omega$ is mainly due to the contact resistances. The measured threshold voltage weakly increases with d for distances approximately below $50\,\mu m$, ranging from $12\,V$ to $16\,V$ and becomes independent of d above this distance. In another hand, the sample threshold voltage is $V_S^* \simeq 60 \pm 20\,mV$ with no clear dependence as a function of d.
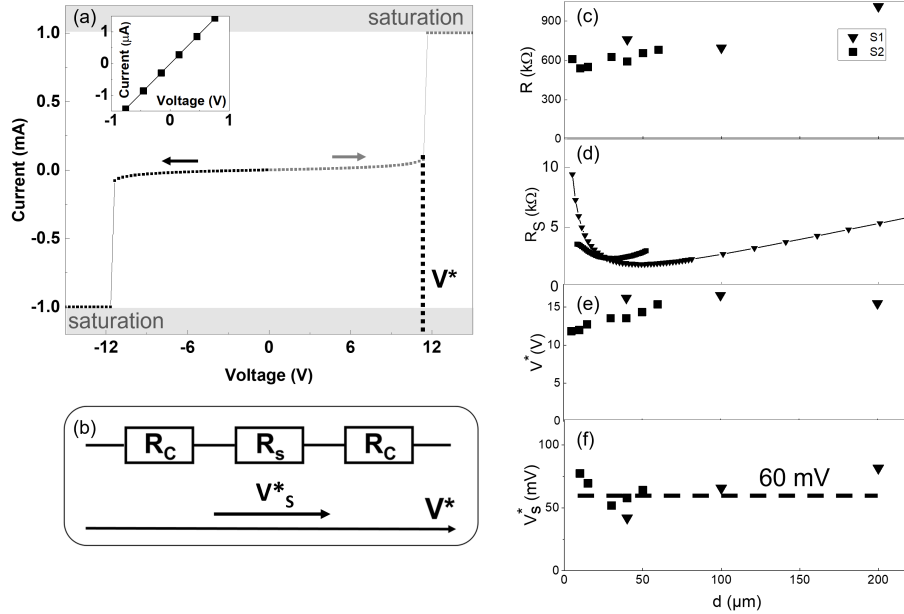

Figure 2. a) Typical current-voltage curve. V^* is the threshold voltage. Arrows indicates the voltage sweep directions. Grey areas indicate the values for which the measured current saturates. Insert: low voltage fit to determine the resistance R. b) Equivalent circuit in the two tip configuration with the contact resistances R_C and sample resistance R_S. V^* is reached for a voltage V_S^*. c,d,e,f) R, R_S, V^* and V_S^* as a function of the interelectrode distance d.

The determination of the electric field threshold E^* from V_S^* depends on the electrodes geometry. According to the literature, the insulator to metal transition occurs as soon as one sample area reaches the threshold electric field [11]. The transition then propagates from near to far up to the creation of a metallic path between the electrodes. E^* then corresponds to the maximal value of the electric field seen locally by the sample for an applied voltage $V = V_S^*$.

Figure 3 presents the simulation of the distribution of the electrical field in the sample, for an applied voltage of $60\,mV$ corresponding to V_S^*. As shown in figure 3a, the electrodes are metal contact defined as disks of radius $r = 1\,\mu m$ at the surface, separated by a distance d. An adaptative mesh as been used to resolve the field distribution. Figure 3b exhibits a typical profile of the electric field along the direction of the applied electric field, at the surface and at $500\,nm$ below. Three characteristic electric fields are labeled E_D, E_E and E_M in the figure. E_D corresponds to a divergence of the electric field at the so called triple point, because it is the junction of the sample, electrode and vacuum. E_E is located below the electrode, at the contact center, and E_M is in the middle of the interelectrode distance.

One could attribute the threshold value E^* to the electric field found at the diverging point E_D. However, we believe that E_D is not the relevant electric field, principally because our experiments show a reproducible value for the voltage threshold, independent of the probe-sample contact. In contrast E_D is expected to depends strongly on the contact geometry with
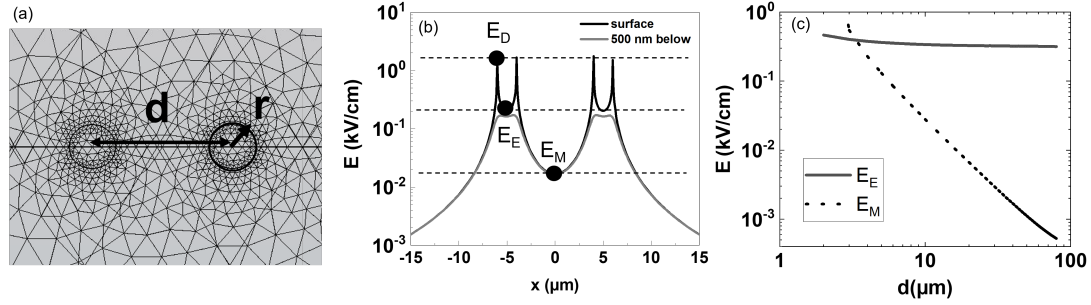
Figure 3. Comsol simulations of the electric field map in the sample for an applied voltage of $60\,mV$ a) Electrode geometry and adaptive mesh used for the simulations. d is the interelectrode distance and $r = 1\,\mu m$ is the radius of the metallic disks corresponding to the contacts. b) Electric field profile at the surface and 500 nm below. c) E_E and E_M as a function of d.

minimal values for obtuse angle contacts [12]. We rather attribute the threshold electric field to E_E, which is the maximum electric field point as soon as the divergences are excluded. Indeed, E_E corresponds to a plateau as shown figure 3b and its value varies slowly when going below the sample surface. E_E is also independent of the interelectrode distance, as shown in Figure 3c. This is compatible with the literature, because the electric field threshold is expected to be an intensive parameter. According to this analysis, we find $E^* = E_E \simeq 0.2\,kV/cm$, which compares well with the value of approximately $0.1\,kV/cm$ at ambient temperature deduced from [5]. In complement, figure 3c shows a change of regime below $d < 3\mu m$, where an increase of the electric field is expected when the electric field E_M between the electrode becomes preponderant.

Conclusion

The resistive switching probed at the surface of $GaMo_4S_8$ has been rationalized using Comsol simulations. The values obtained for the resistivity and the electric field threshold compare well with the literature. This study provides a framework for analysis of the resistive switching as a function of the electrodes geometry.

Acknowledgments

References

[1] Takagi H and Hwang H Y 2010 *Science* **327** 1601–02
[2] Basov D N, Averitt R D and Hsieh D 2017 *Nat. Mater.* **16** 1077–88
[3] Wang Y, Kang K M, Kim M, Lee H S, Waser R, Wouters D, Dittmann R, Yang J J and Park H H 2019 *Materials Today* **28** 63–80
[4] Janod E. *et al. Adv. Func. Mater.* 2015 **25** 6287-305
[5] Diener P *et al.* 2018 *Phys. Rev. Lett.* **121** 016601
[6] Adda C *et al. J. Appl. Phys.* 2018 **124** 152124
[7] Dubost V, Cren T, Vaju C, Cario L, Corraze B, Janod E, Debontridder F. and Roditchev D 2013 *Nano Lett.* **13** 3648-53
[8] Durand C, Capiod P, Berthe M, Nys JP, Krzeminski C, Stiévenard D, Delerue C and Grandidier B 2014 *Nano Lett.* **14** 5636–40
[9] Miccoli I, Edler F, Pfnür H and Tegenkamp C 2015 *J. Phys.: Condens. Matter* **27** 223201
[10] Oka T and Nagaosa N 2005 *Phys. Rev. Lett.* **95** 266403
[11] Stoliar P, Cario L, Janod E, Corraze B, Guillot-Deudon C, Salmon-Bourmand S, Guiot V, Tranchant J, and Rozenberg M 2013 *Adv. Mater.* **25** 3222-6
[12] Bayer C, Baer E, Waltrich U, Malipaard D and Schletz A 2015 *IEEE Trans. Dielectr. Electr. Insul.* **22** 257-65